PROCEEDINGS, Twenty-Seventh Workshop on Geothermal Reservoir Engineering
Stanford University, Stanford, California, January 28-30, 2002
SGP-TR-171

MAGNETOTELLURIC INTERPRETATION OF THE KARAHA BODAS GEOTHERMAL FIELD INDONESIA

Imam Raharjo[1,4], Phil Wannamaker[2], Rick Allis[3], David Chapman[1]

[1]Dept. of Geology and Geophysics, University of Utah, Salt Lake City
[2]Energy and Geosciences Institute, University of Utah, Salt Lake City
[3]Utah Geological Survey, Salt Lake City
[4]Pertamina Geothermal, Jakarta
iraharjo@mines.utah.edu

ABSTRACT

The Karaha Bodas Field is a vapor-type geothermal system having a temperature of up to 350°C. The reservoir is hosted in a volcanic environment comprises of tuff breccias with minor andesite lavas, and quartz diorite intrusions. Based on the surface thermal distribution the system might occupy an area of 5x13 km^2. One hundred and eighty magnetotelluric (MT) stations recorded in 1996 and 1997 were used to assess the clay cap extension. One -dimensional MT interpretations were performed. A north-south MT profile crossing the entire field was chosen to show the extent of the possible resources. The profile shows a very thick conductive layer (1-10Ω m) extending 7 km northward from the Bodas Crater. The thickness of the conductive layer is about 1000-1200 m having a base at about 200-300 meters above sea level. Between 7-12 km north of the crater the layer thins (to 700 m), and the resistivity increases slightly to 14Ω m. The interface between the conductive layer and the underlying layer also coincides with fluid loss zones during drilling operation. This observation suggests that the conductive layer is still the clay cap of the reservoir. Other, and more complex, resistivity structures caused by multiple hydrothermal processes are not imaged by the MT data. At a distance of 12 km from the crater the conductive layer vanishes. Some thermal springs and steaming ground also occur, suggesting the northern boundary of the system.

INTRODUCTION

The Karaha Bodas Field is a vapor-dominated system, located in West Java, Indonesia. The temperature of the reservoir varies from about 250° to up to 350°C. The hottest part of the field is the Bodas Area in the south. The temperature trend gradually decreases northward down to probably 250° in the Karaha Block on the north side. Consequently, the main thermal surface activities over the area consist of fumaroles, an acidic lake, and hot springs in Bodas Area, while in the Karaha Area altered ground associated with steaming ground occur together with some thermal springs. Overall, the reservoir temperature is hotter than the adjacent vapor geothermal field Kamojang with temperature to 225°C. The shallow hydrothermal circulation combined with the condensed steam on the upper part of the reservoir forms a clay cap. This acts as a conductive blanket that covers the entire reservoir. In a mountainous area like this, topography drives the shallow hydrothermal circulation. This paper is a preliminary effort to image the gross resistivity structure of the field and to delineate the possible reservoir boundary.

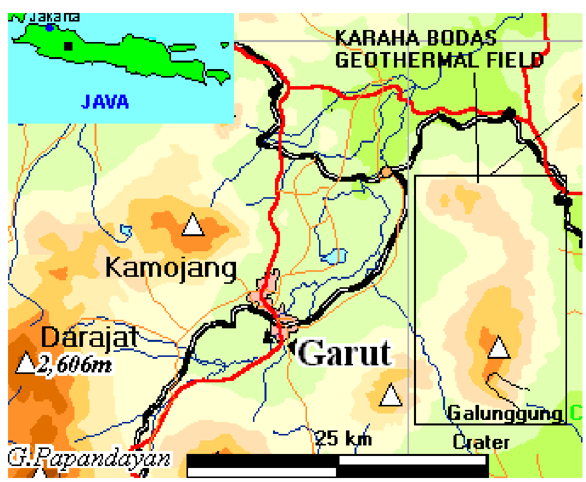

Figure 1. Location Map of the Karaha Bodas Geothermal Field. Darajat (55 MW) and Kamojang (140 MW) are vapor-dominated reservoirs.

METHOD

We use magnetotellurics delineate the extent of possible resources. One-dimensional forward and inverse modeling is employed. These results are compared to downhole temperature measurements, the surface thermal manifestations, and the depth of circulation loss during drilling.

PREVIOUS WORK

Geophysical surveys that have been completed include gravity, DC Schlumberger, and Magnetotellurics. Twenty six wells have also been drilled. Papers discussing Karaha include magnetotellurics interpretation (GENZL, 1997), evolution of the field (Allis and Moore, 2000), and the Karaha hydrothermal system (Allis, et.al., 2000). Karaha is a two hours drive from Bandung making this field area very accessible. It sits on the north flank of the Galunggung which erupted in 1982 (Figure 1).

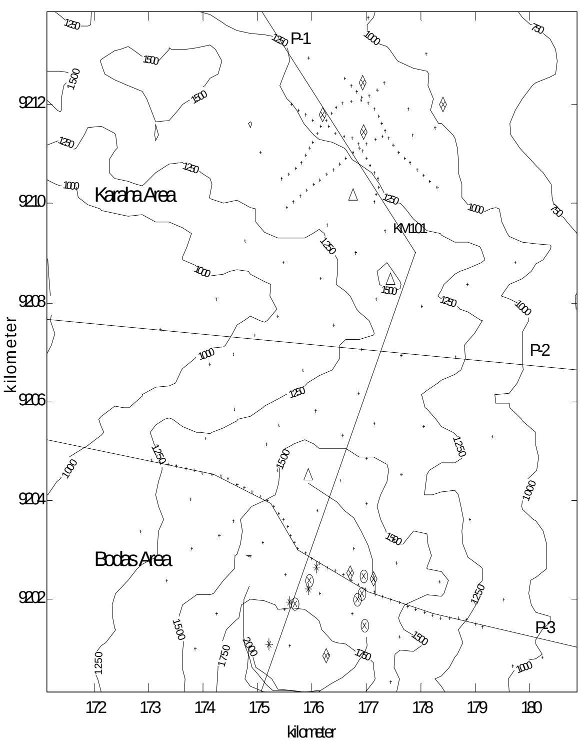

Figure 2. Situation map of the field. The contour interval is 250. Fumaroles are shown as stars, thermal springs are shown as circles and diamond shape marks. MT sites are shown as plus marks .

GEOLOGY

Geologic Mapping (Ganda, et. al. 1985) and the wellbore data (EGI, 2001) indicate that the entire field is covered by Quarternary volcanic debris interlayered with minor andesite lavas having thickness of up to 100 m. Some dark colored lake sediments were also encountered during drilling and are dated back to be as old as 6000 years (Moore, 2001, private communication). Quartz diorite intrusions are found in the center and north part of the field at an elevation of about 1 km below sea level. These intrusions together with another magmatic chamber beneath Galunggung Volcano are believed to provide the heat source for the field. At lower elevation Sedimentary deposits are found.

The field is characterized by a prominent north-south volcanic ridge, comprising several volcanic peaks.

MAGNETOTELLURIC THEORY

The magnetotellurics (MT) method is a natural-field electromagnetic method utilizing the field induced by magnetospheric or ionospheric current. Since the source is far away, the field can be treated as a plane wave (Zhdanov and Keller, 1998). The second theorem of the Maxwell equation states that

$$\text{curl } E = -\partial B/\partial t, \tag{3.1}$$

where E is an Electric field and B is magnetic field.

Since a plane wave is utilized (E_Z=0) and MT frequency used is usually low, the equation can be expanded into

$$\begin{bmatrix} dx & dy & dx \\ \partial/\partial x & \partial/\partial y & \partial/dz \\ E_x & E_y & 0 \end{bmatrix} = -i\varpi\mu_0 (H_x d_x + H_y d_Y) \tag{3.2}$$

where $B=\mu_0 H$. (3.3)

Recall that vertical plane wave does not have derivatives in x and y direction. By expanding equation (3.2), we end up with two independent equations :

$$H_x = -\frac{1}{i\varpi\mu_0}\frac{dE_y}{dz}, \text{ and } \; H_y = \frac{1}{i\varpi\mu_0}\frac{dE_x}{dz}. \tag{3.4}$$

From this point one can apply a solution of Helmholtz operator to the equations to yield a simple relationship between electric field (E) and magnetic field (H) to its impedance (Z)

$$Z_{xy} = \frac{E_x(z)}{H_y(z)}, \text{ and } \; Z_{yx} = -\frac{E_y(z)}{H_x(z)}. \tag{3.5}$$

Furthermore, one can derive the corresponding apparent resistivity which are

$$\rho_{xy} = \frac{1}{\varpi\mu_0}|Zxy|^2, \quad \text{and} \quad \rho_{yx=} \frac{1}{\varpi\mu_0}|Z_{yx}|^2. \quad (3.6)$$

In this general case, electric and magnetic fields are a function of conductivity (σ), dielectric permitivity (ε), and magnetic permeability (μ) of the material. This relationship can be formulated as

$$\{E, H\} = A(\sigma, \varepsilon, \mu) \quad (3.7)$$

where A is a forward operator applied into σ,ε, and μ. Keep in mind that σ is just simply $1/\rho$. The corresponding inverse problem is

$$\{\sigma, \varepsilon, \mu\} = A^{-1}\{E, H\} \quad (3.8)$$

In most presentations, E and H are usually combined together as an apparent resistivity ρ_a, ρ_{xy} or ρ_{yx}. This is a nonlinear problem, therefore finding the forward operator A is sometimes rather complicated. One of many simplest one-dimensional forward operators is the reflectivity coefficient, R_N (Zhdanov, and Keller, 1998). The result is used to develop a forward model, as followings.

Given N layers, the reflectivity coefficient of the most bottom interface is

$$R_1 = 1. \quad (3.9)$$

The reflectivity coefficients for the next j layers (R_2) to the earth surface (R_N) can be calculated as,

$$R(j) = \frac{1 - K(j)e^{(-2ikud(N-j+1))}}{1 + K(j)e^{(-2ikud(N-j+1))}} \quad (3.10)$$

where
$$K(j) = \frac{1 - \frac{ku}{kl}R(j-1)}{1 + \frac{ku}{kl}R(j-1)}; \quad (3.11)$$

$$ku = \sqrt{(i\varpi\mu_0\sigma(N - j + 1))};$$
$$kl = \sqrt{(i\varpi\mu_0\sigma(N - j + 2))}, \quad (3.12)$$

and d is thickness of the layers. At the very bottom interface the K(1) is also equal to one. To obtain a series of ρ_a curve, these equations should be looped over the desired period, as shown in the attached MATLAB codes (Appendix-1).

The inversion code uses a least-squared method which utilizes Marquadt's stabilizer (Wannamaker, 1990). The method is a special case in Tikhonov's parametric function. If we recall the forward operator A, and apply it to a model m, then Am is the predicted data. The idea of the least-squared method is minimize the difference between the observed data (d) with the predicted data Am. This value is called misfit function,

$$f(m) = \left\| Am - d)^2 \right\| = (Am - d, Am - d) = \min. \quad (3.13)$$

Using matrix notation this equation can be rewritten as

$$f(m) = (Am - d)^T (Am - d) = \min \quad (3.14)$$

After applying variational calculus to equation (3.14), the solution gives the model m_o,

$$m_0 = (A^T A)^{-1} A^T d \quad (3.15)$$

In most cases the inverse of ($A^T A$) does either not exist or close to singular. Therefore Tikhonov (Zhdanov and Keller, 1998) introduced a stabilizer coefficient α, an apriori model m_{apr}, and some weighting matrices of data (W_d) and model (W_M) that give more stable solution,

$$m_\alpha = (A^T W_d^2 A + \alpha W_m^2)^{-1} (A^T W_d^2 + \alpha W_m^2 m_{apr}). \quad (3.16)$$

Marquadt method simplifies W_d=I and W_M=I, m_{apr} =0, and uses singular value decomposition to represent the forward operator A as $(UQV)^T$. In this case U is a column-orthogonal matrix, Q is a diagonal matrix, and V is a square orthogonal matrix. The solution is then

$$m_\alpha = (A^T A + \alpha I)^{-1} A^T d = V\left[\frac{1}{Q^2 + \alpha I}\right] Q^T U^T d. \quad (3.17)$$

Because this is non linear problem, the least-squared solution has to be iterated until the misfit reaches a desirable error.

DATA AVAILABLE

On behalf of Karaha Bodas Company, in 1996 and 1997 Geosystems undertook MT measurements in the field. Half of the stations were scattered over the field, and the rest were aligned into 5 dense lines (Figure 2). These data are available through EGI in EDI ASCII format. Remote reference procedure was deployed to minimize error. This yield good quality data, as shown by the plot of the resistivity curves and the corresponding error bars (Figure 5). One hundred and eighty stations were selected for this study. Prior to the interpretation stage, static shift correction have been applied utilizing TDEM data, using a simple MATLAB code.

MT INVARIANT APPARENT RESISTIVITY MAPS

Gross resistivity structure of the field are recognized from resistivity maps. One of these is invariant apparent resistivity map, which is the geometric mean of ρ_{xy} and ρ_{yx} :

$$\rho_{inv} = (\rho_{xy} \times \rho_{yx})^{0.5} \qquad (3.18)$$

Figures 3 and 4 show resistivity maps constructed at periods of 0.25 s and 1.0s, respectively.

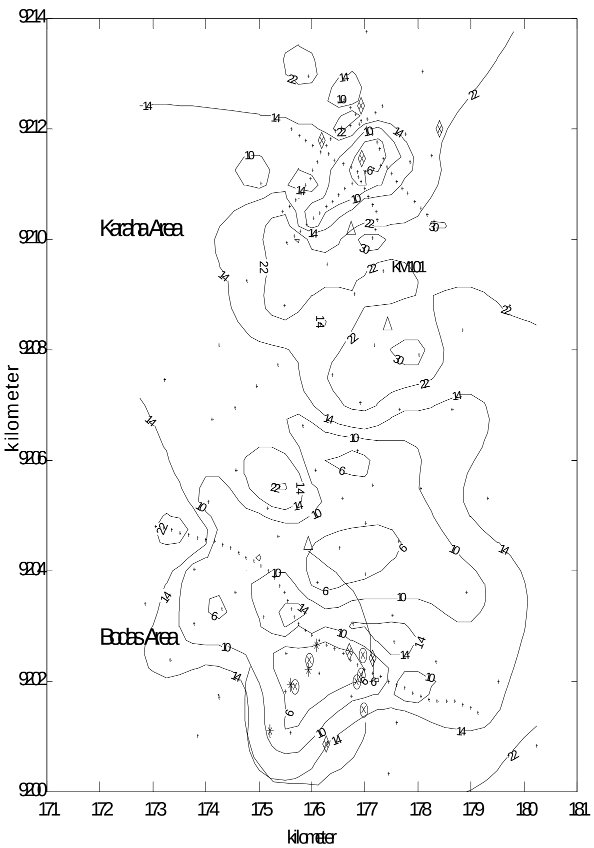

Figure 3. MT invariant apparent resistivity map at a period of 0.25s showing a shallow conductor in the Bodas Area. Contours are in Ohm.m.

A shallow low resistivity zone (<10 Ω.m) is observed in the Bodas Area (Figure 3). The depth of a particular signal in MT can be calculated using the following equation;

$$\delta = 503\sqrt{\rho \times T} \qquad (3.19)$$

where δ is the skin depth in meter and T is the period (1/frequency) of the signal. Hence the skin depth of the contour 10 Ω.m is about 800m. This shallow conductive area might correlate with an argillic type alteration in the upflow zone and its vicinity. The conductor does not extend to the north. There are two resistive spots within the conductive zone in the Bodas Area (Figure 3). These are the signatures of the escaping steam in the Bodas Area.

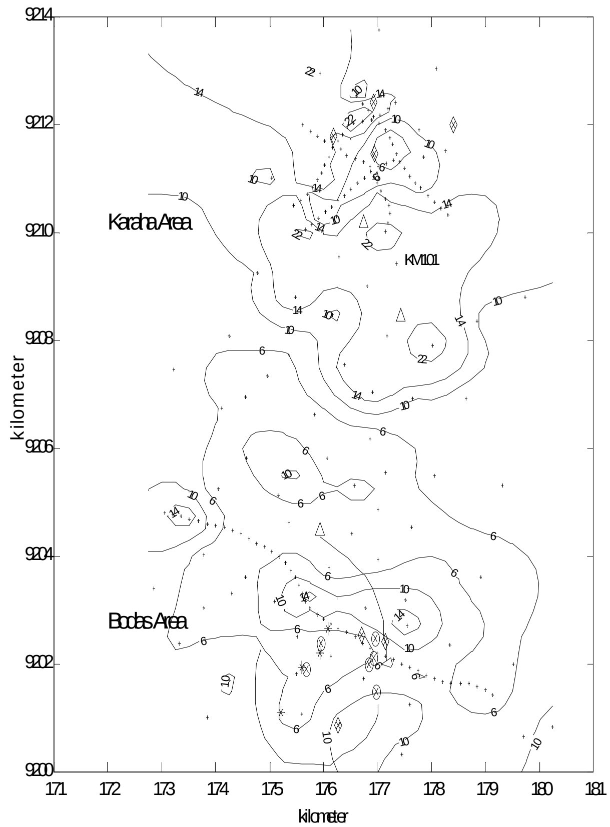

Figure 4. MT invariant apparent resistivity map at a period of 1.0s showing a deeper conductor having a wider coverage. Contours are in Ohm.m. The slightly resistive spot in the Bodas Area is the escaping steam signature.

At greater depth the conductor (<10 Ω.m) becomes wider and covers almost two thirds of the area as shown in Figure 4. The skin depth of the contour 10 Ω.m at this period is about 1600m. The extent of this layer might be controlled by deeper circulating hydrothermal fluids driven by topography, or deeper argillic alteration. Surrounding sedimentary rocks (2-D or even 3-D) might also contribute to this layer. The steam signature in the Bodas area consistently shows up on the resistivity map.

ONE-DIMENSIONAL MODELING

In order to model subsurface resistivity structure slices over the field, one-dimensional MT modeling is employed. The MT data at site KM101 located in Karaha Area is used as an example in this paper (Figure 5).

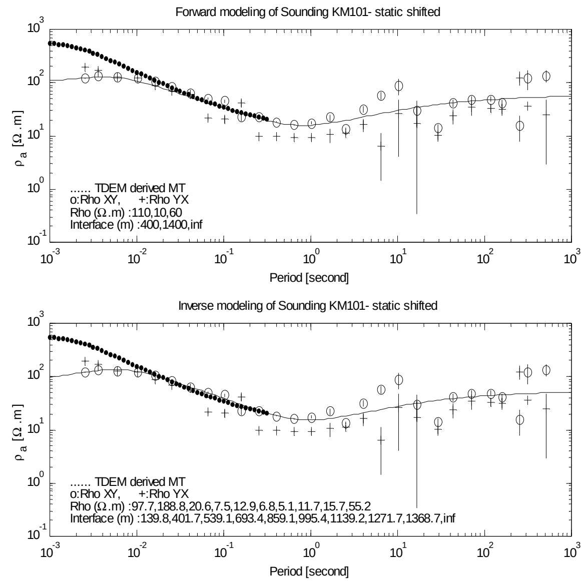

Figure 5. One-dimensional forward and inverse modeling of the MT site KM101 located in the Karaha Area.

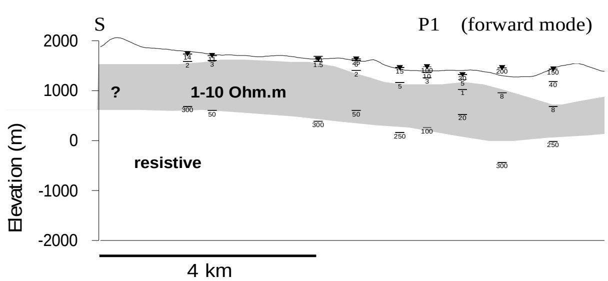

Figure 6. Profile-1 showing a conductive layer having a tongue shape vanishes to the north from forward modeling.

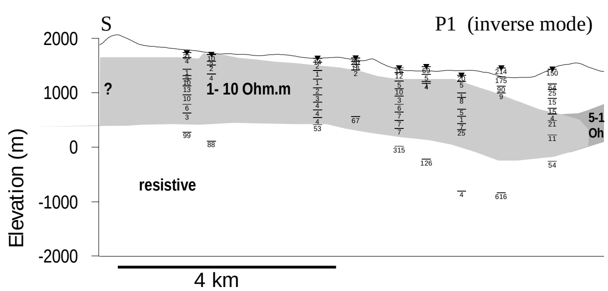

Figure 7. Profile-1 showing a conductive layer having a tongue shape vanishes to the north from inverse modeling

The MT record from this site shows a 1-D environment. i.e. there is not a severe split between ρ_{xy} and ρ_{yx} . The forward and inverse models of the curve are shown in Figure 5. In general, the curves suggest a three layers structure, comprise of resistive-conductive-resistive layers. The forward model shows a thick conductive layer (10Ω.m, 1000m) at a depth of about 300m. The inverse model which employs ten layers shows gradually-changing layers having a minimum value of about 5 Ω.m. The total thickness of the conductive layers is about 900m.

Forward and inverse modeling was undertaken to interpret all MT sites. Three sections were then constructed having directions shown in Figure 2. Profile-1 is running north-south and is displayed in both forward and inverse model. Profile-2 and Profile-3 are run west-east and are displayed in inverse models only. Before discussing these profiles in detailed, it is important to understand the geohydrology of the system.

Topography plays important role in groundwater movement in a mountainous area, i.e. the hydraulic gradient in the flank drives the deeper groundwater movement. Fortunately one can draw a rough groundwater movement based on the topographic terrain, since the shape of the water table is usually concordant with the topography. Following this rule, hydrothermal fluid arising from the deeper part of the upflow zone will flow to the flank of the volcano. Hot, warm, or even coldsprings on the volcano flanks are the evidence of downhill fluid movement. As a consequence, a tongue shape alteration from upflow to the outflow zone is common in andesitic hosted geothermal system. If this hydrothermal fluid movement has enough time to alter the host rock, one might able to map the associated low resistivity layer.

The forward and inverse models on the Profile-1 generally agree, both have a 12 km long conductive layer. The thickness from the inverse modeling is somewhat greater. The layer has a tongue shape which vanishes to the north. Based on the inverse modeling, the thickness of the layer is about one 1000-1200 meter in the Bodas Area. The top of layer deepens to the north, and then goes up again to reach the surface in the north end. The thickness is also decreasing to about 700 m. The resistivity values in the conductive layer can also be grouped into south layer and north layer. The south layer resistivity ranges from 1 to 10 Ω.m, while the north layer resistivity ranges from 5 to 14 Ω.m .

The tips of the layer in the west east direction are not recognized from the corresponding profiles, due to the lack of data. Figures 8 and 9 show the two profiles. However a downhill trend conductor can be clearly seen from the profiles. Surprisingly the thickness of the layer in the flank is thicker in the north profile compared to the south profile. This leads to a preliminary guess that the north part has more downhill flow compared to the south. Integration and interpretation with other methods are needed to determine reservoir boundaries in west east direction not discussed in this paper.

If we recall the profile-1 and compare the extent of the layer with other subsurface data, such as the temperature profile, the depth of circulation loss zone, and the thermal manifestations, some interpretation can be made. Figure 10 shows the extent of the conductive layer superimposed on some subsurface data. At the Bodas Area the conductive layer is concordant with the temperature region of 100-260°C. The upper part of the region mostly comprises of argillic type alteration (Moore, 2001. private comm.). This region has a low conductivity of 1-10 Ωm. If we recall that the Bodas crater is the upflow zone of the field (Allis, et. al., 2000), then extent of the layer from the upflow zone is about 7 km to the north. The base of the layer is about 200-300 meter above sea level. This range coincides with the top loss zone of the reservoir. This implies that the layer is still the clay cap of the reservoir. Keep in mind that the resistivity of a vapor reservoir is usually slightly higher than the resistivity of the clay cap. The layer becomes thinner (to 700 m) as it goes from 7 to 12 km northward in the Karaha Area. The resistivity range of the layer also increases slightly to 5-14Ω m. This might be related to the fact that alteration process in the Karaha Area is not as vigorous as those in Bodas area. At a distance of 12 km from the Bodas crater the layer vanishes. Some cold springs and altered ground also occur, suggesting the northern boundary of the system. The most likely geothermal reservoir is shown in the Figure 10.

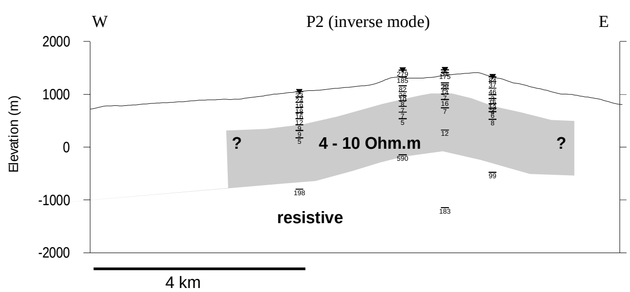

Figure 8. Profile-2 showing a conductive layer in the west east direction from inverse modeling.

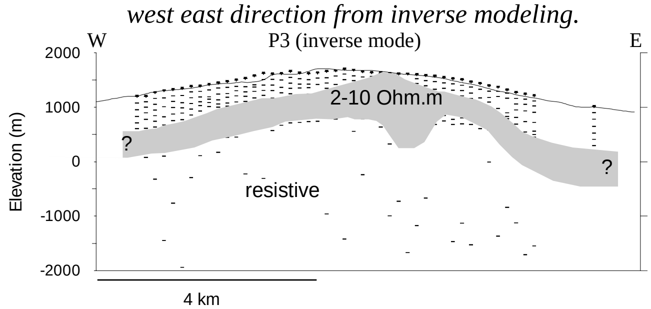

Figure 9. Profile-3 showing a conductive layer in the west east direction from inverse modeling

Figure 10. The extent of the conductive layer superimposed on Allis et.al. model, 2000.

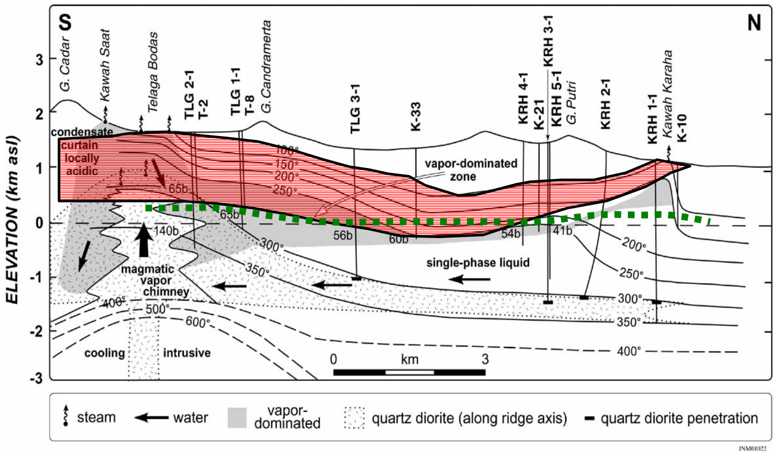

The layer is shown in shaded region. The dotted line is the depth of the top loss zone during drilling.

CONCLUSIONS AND FURTHER WORK

The following conclusions summarize the discussion,

- The extent of the conductive layer in the north-south profile can be used to delineate the northern boundary
- In general the conductive layer coincides with the temperatures of 100-260°C
- The base of the conductor is concordant with the depth pf circulation loss zone, suggesting that the layer is still acting as the cap of the system.

To obtain a better image of the resistivity structure of Karaha, we plan to perform 2-D MT modeling using a finite element method Program (Wannamaker, 1990).

ACKNOWLEDGMENT

The principal author would like to thank to the EGI for providing the data, and to the World Bank through the JJ/WBGSP for providing the fellowship at the University of Utah.

REFERENCES

Allis, R., Moore, J.N. (2000), "Evolution of Volcano-Hosted Vapor-Dominated Geothermal Systems", *Geothermal Resources Council Transaction, Vol.24*, 211-216.

Allis, R., et.al. (2000), "Karaha-Telaga Bodas, Indonesia: A Partially Vapor-Dominated Geothermal Systems", *Geothermal Resources Council Transaction, Vol.24*, 217-222.

GENZL (1997), "Survey Report, Karaha Telaga Bodas MT Survey - 1997", prepared for Karaha Bodas Co., unpublished, Ganda, S., Boedihardi, M., Rachman, A., and Hantono, D. (1985), “Geologi Daerah Kawah Kamojang dan Sekitarnya, Kabupaten Tasikmalaya, Garut, Majalengka, dan Sumedang, Propinsi Jawa Barat”, *Divisi Geothermal, Pertamina Pusat*.

EGI, (2001), “Downhole Karaha Data”, unpublished, *Energy and Geoscience Institute*,

Wannamaker, P.E. (1990), "Finite Element Program for Magnetotelluric Forward Modeling and Parameterized Inversion of Two-Dimensional Earth Resistivity Structure”, *University of Utah Research Institute,* 41 pages.

Zhdanov, M.S., Keller, G.V. (1998), "The Geoelectrical Methods In Geophysical Exploration”, *Method In Geochemistry and Geophysics, 31*, 261-346.

APPENDIX-1

```
% MT Rn - code to run a 1-D MT modeling
clear all;
Rho=[100 10 1000];
depth=[500 1000]; % interface depth
nlayer=length(Rho);
d(1)=depth(1); % thickness
for j=2:nlayer-1,
   d(j)=depth(j)-depth(j-1);
  end;
maxcount=81;
u0=4*pi*10^-7;
xplot=zeros(maxcount,1);
R=zeros(nlayer,1);
K=zeros(nlayer,1);
To=zeros(maxcount,1);
Rn=zeros(maxcount,1);
Ph=zeros(maxcount,1);
% --- for a series of frequencies
pow=-3;
for n=1:maxcount;
  To(n)=10^(pow);pow=pow+.1;
end

R(1)=1;K(1)=1;
for nf=1:maxcount, % Loop over a series of frequencies
  w=2*pi/To(nf);
   for n=2:nlayer,
    ku=(i*w*u0/Rho(nlayer-n+1))^.5;
    kl=(i*w*u0/Rho(nlayer-n+2))^.5;
    K(n)=(1-ku/kl*R(n-1))/ ...
        (1+ku/kl*R(n-1));
R(n)=(1-K(n)*exp(2*i*ku*d(nlayer-n+1)))/ ...
 (1+K(n)*exp(2*i*ku*d(nlayer-n+1)));
   end;
   Rn(nf)=Rho(1)*abs(R(nlayer)^2);
end;
loglog(To,Rn,'b.')
axis([1E-3 1E3 1E0 1E4]);
xlabel('T second');
ylabel('\rho_a_p_p \Omegam');
title('Apparent resistivity for an n-layered earth ').
```